



**HAL**  
open science

## Development of a NiW in-situ diffusion barrier on a fourth generation nickel-base superalloy

Eric Cavaletti, Stéphane Mercier, Denis Boivin, Marie-Pierre Bacos, Pierre Josso, Daniel Monceau

### ► To cite this version:

Eric Cavaletti, Stéphane Mercier, Denis Boivin, Marie-Pierre Bacos, Pierre Josso, et al.. Development of a NiW in-situ diffusion barrier on a fourth generation nickel-base superalloy. *Materials Science Forum*, 2008, 595-598, pp.23-32. 10.4028/www.scientific.net/MSF.595-598.23 . hal-04473387

**HAL Id: hal-04473387**

**<https://hal.science/hal-04473387v1>**

Submitted on 22 Feb 2024

**HAL** is a multi-disciplinary open access archive for the deposit and dissemination of scientific research documents, whether they are published or not. The documents may come from teaching and research institutions in France or abroad, or from public or private research centers.

L'archive ouverte pluridisciplinaire **HAL**, est destinée au dépôt et à la diffusion de documents scientifiques de niveau recherche, publiés ou non, émanant des établissements d'enseignement et de recherche français ou étrangers, des laboratoires publics ou privés.



## Open Archive Toulouse Archive Ouverte (OATAO)

OATAO is an open access repository that collects the work of Toulouse researchers and makes it freely available over the web where possible.

This is an author-deposited version published in: <http://oatao.univ-toulouse.fr/>  
Eprints ID : 2348

**To link to this article :**

URL : <http://dx.doi.org/10.4028/www.scientific.net/MSF.595-598.23>

**To cite this version :** Cavaletti, Eric and Mercier, Stéphane and Boivin, Denis and Bacos, M.P and Josso, P. and Monceau, Daniel ( 2008) [\*Development of a NiW in-situ diffusion barrier on a fourth generation nickel-base superalloy.\*](#) Materials Science Forum, vol. 595 - 598 . pp. 23-32. ISSN 0255-5476

Any correspondence concerning this service should be sent to the repository administrator: [staff-oatao@inp-toulouse.fr](mailto:staff-oatao@inp-toulouse.fr)

# Development of a NiW *in-situ* diffusion barrier on a fourth generation nickel-base superalloy

E. Cavaletti<sup>1,a</sup>, S. Mercier<sup>1,b</sup>, D. Boivin<sup>1,c</sup>, M.-P. Bacos<sup>1,d</sup>, P. Josso<sup>1,e</sup>, D. Monceau<sup>2,f</sup>

<sup>1</sup>ONERA, Metallic Materials and Processes Department, BP72, 92322 Chatillon cedex, France

<sup>2</sup>CIRIMAT CNRS-INPT-UPS, ENSIACET 31077 Toulouse, France

<sup>a</sup>eric.cavaletti@onera.fr, <sup>b</sup>sebastien.mercier@onera.fr, <sup>c</sup>denis.boivin@onera.fr,

<sup>d</sup>marie-pierre.bacos@onera.fr, <sup>e</sup>pierre.josso@onera.fr, <sup>f</sup>daniel.monceau@ensiacet.fr

**Keywords:** Thermal barrier system, diffusion barrier, secondary reaction zone, bondcoating, diffusion, electrolytic coating

**Abstract.** A diffusion barrier based on a NiW electrolytic coating has been developed to limit interdiffusion between a Ni-base superalloy (MCNG) and a  $\beta$ -NiAl bondcoating. Isothermal oxidation tests of 50h at 1100°C confirmed that W-rich layer formed with NiW coating modifies the oxidation behaviour of the bondcoat and limits interdiffusion. The diffusion barrier reduced  $\beta$ -NiAl  $\rightarrow$   $\gamma'$ -Ni<sub>3</sub>Al transformation in the bondcoating and prevented SRZ formation.

## Introduction

For a thermal barrier system exposed at high temperature, interdiffusion occurs between the superalloy and the nickel aluminide protective coating, which can have fatal consequences on the service life of the system. Firstly, it increases the extent of Al depletion from the coating and accelerates the  $\beta$ -NiAl  $\rightarrow$   $\gamma'$ -Ni<sub>3</sub>Al transformation. Secondly, elements from the superalloy diffuse through the aluminide bondcoating up to the thermally grown oxide scale (TGO) and some of them have detrimental effects on the oxide-scale adherence. Thirdly, interdiffusion leads to the creation of detrimental secondary reaction zones (SRZ) [1] at the coating/superalloy interface.

Diffusion barrier coatings have been developed [2, 3] to limit this interdiffusion phenomenon. Nevertheless the deposit of a dense diffusion barrier before aluminisation reduces nickel diffusion from the superalloy which permits to create the  $\beta$ -NiAl coating. So a Ni film is generally electroplated on dense diffusion barrier [2]. To avoid this electroplating step, a duplex electrolytic Co-NiW coating was developed [4] as a diffusion barrier. The nickel within the NiW coating participates with the nickel of the superalloy to form the  $\beta$ -NiAl bondcoating. Co stabilizes the  $\gamma$  phase of the superalloy and slows down the matrix inversion ( $\gamma/\gamma' \rightarrow \gamma'/\gamma$ ) leading to the creation of SRZ [5]. W in the NiW coating forms definite compounds with the refractory elements of the superalloys. The size of these compounds increase during service by dissolution of alloying elements and coalescence to slow down interdiffusion kinetics. Fig. 1 shows the steps of the Co-NiW diffusion barrier fabrication.

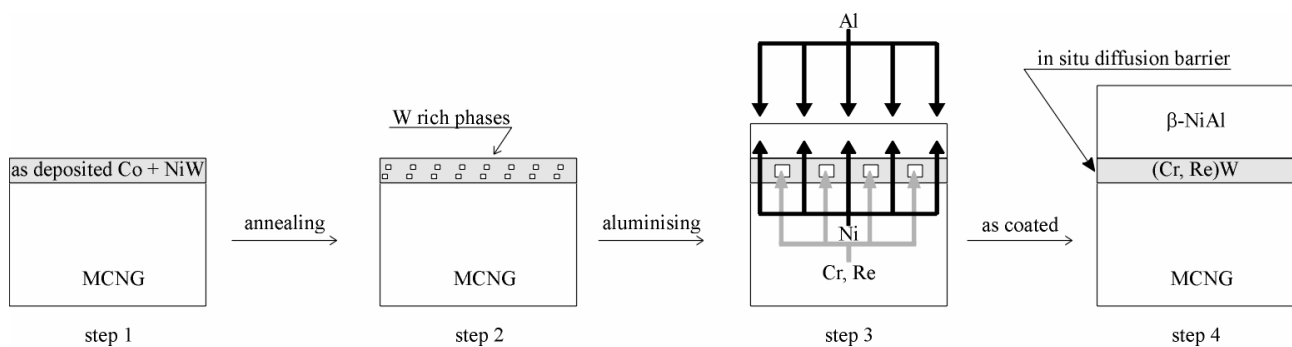


Fig. 1. Principle of a Co-NiW in situ diffusion barrier formation

The aim of this work was to study the development of this diffusion barrier in the case of a Ni-base superalloy protected by a nickel aluminide diffusion coating. In this initial study, the role of Co was not investigated in order to simplify the system. Therefore, the efficiency of a diffusion barrier (DB) based on a simple NiW barrier coating annealed 16h at 1100°C before aluminisation will be discussed here.

## Materials and Experimental Procedures

**Materials.** The test specimens used for this study were 11mm diameter and 2mm thick pieces of MCNG superalloy. The nominal composition of this alloy developed by ONERA [6] is given in Table.1. The  $\beta$ -NiAl bondcoatings were obtained by low activity vapour phase Al-cementation process.

Table.1 Chemical composition of MCNG superalloy in wt% [6]

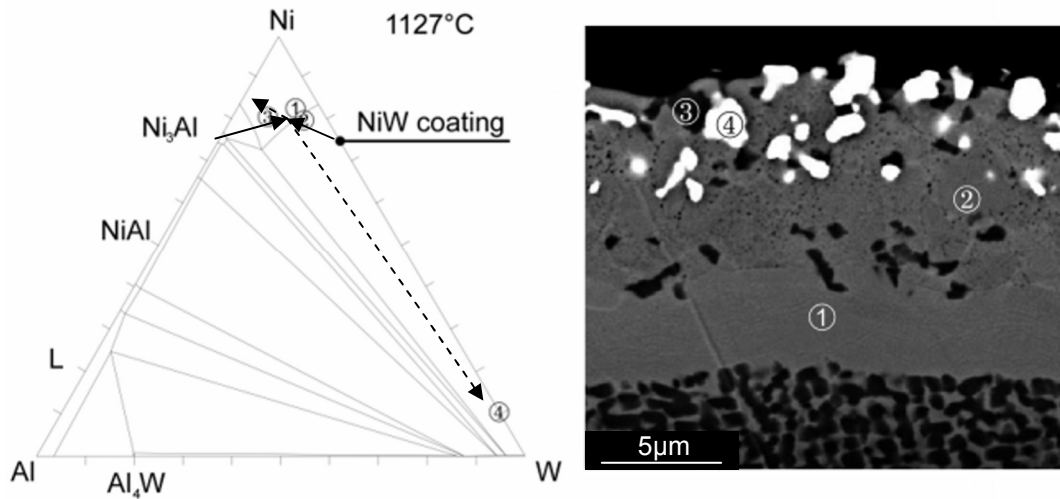
| Ni   | Cr  | Mo | Re  | Ru  | W   | Al  | Ti  | Ta | Others             |
|------|-----|----|-----|-----|-----|-----|-----|----|--------------------|
| Bal. | 3,9 | 1  | 4,1 | 4,1 | 5,1 | 5,9 | 0,5 | 5  | Hf: 0,1<br>Si: 0,1 |

**NiW Electrolytic Coating.** The DB involved in this paper is based on a NiW electrolytic coating. The composition of the associated electrolytic bath was 20g.l<sup>-1</sup> of NiSO<sub>4</sub> 7H<sub>2</sub>O, 100g.l<sup>-1</sup> of NaWO<sub>4</sub> 2H<sub>2</sub>O and 66g.l<sup>-1</sup> of C<sub>6</sub>H<sub>8</sub>O<sub>7</sub> H<sub>2</sub>O. This bath was used at pH=7.5 and a temperature of 70°C. At a current density of 15A.dm<sup>-2</sup>, it took 10min to form a 7 $\mu$ m NiW thick coating with a composition of Ni (75-80 at%) and W (20-25 at%).

**Isothermal Oxidation Tests.** Isothermal oxidation tests were performed on as-processed coated specimens in a Setaram TGA24S thermobalance for 50h in dry synthetic flowing air at 1100 °C. Mass gain curves were analyzed by local fitting to a general parabolic law [7].

## Diffusion Barrier System Fabrication

**Annealing of the NiW Coating.** The DB studied in the present paper is based on a NiW electrolytic coating annealed 16h at 1100°C before aluminisation.



| at% | Al    | Ti   | Cr   | Ni    | Mo   | Ru   | W     | Re   |
|-----|-------|------|------|-------|------|------|-------|------|
| (1) | 5.53  | 0.25 | 1.34 | 78.92 | 0.59 | 1.46 | 11.15 | 0.76 |
| (2) | 5.21  | 0.22 | 0.56 | 77.88 | 0.65 | 1.13 | 14.34 | 0.00 |
| (3) | 12.24 | 0.40 | 0.14 | 78.03 | 0.23 | 0.64 | 0.80  | 0.51 |
| (4) | 0.00  | 0.00 | 0.30 | 9.79  | 0.24 | 0.00 | 88.18 | 1.49 |

Fig. 1. Cross section of the NiW coating annealed 16h at 1100°C and chemical concentrations of the different phases reported on a NiAlW ternary phase diagram [8]

After 16h of annealing, a 5µm thick superalloy layer with a  $\gamma/\gamma'$  microstructure had been transformed to a W-enriched  $\gamma$ -Ni solid solution (Fig. 2-(1)). The Al from the  $\gamma'$  phase diffused to the Ni<sub>75</sub>W<sub>25</sub> coating to form Al-rich  $\gamma$ -Ni (3) and W (4) in a W-rich  $\gamma$ -Ni matrix (2). These phases had chemical concentrations in accordance with the ternary phase diagram and suggested a diffusion path as seen in Fig. 2. Ru and Cr diffused from the superalloy (1.46at% and 1.34at% in (1) and 1.13at% and 0.56at% in (2) respectively).

### As aluminised samples

**Without diffusion barrier.** A cross-section of aluminised MCNG (Fig. 2 - a) presents three different zones above the MCNG superalloy. First a secondary reaction zone (SRZ) in which the  $\gamma/\gamma'$  microstructure of the superalloy has been modified to a  $\gamma'/\gamma$  microstructure with TCP. This modification seems to be driven by Al diffusion from the bondcoating [6, 9]. For this as-aluminised specimen the developed SRZ occupied about 50% of the superalloy periphery and was about 10-15µm in depth. Above this SRZ there was the interdiffusion zone (IDZ) composed of refractory element (Cr, Re) precipitates in a matrix. Above the interdiffusion zone (IDZ), the  $\beta$ -NiAl protective coating had an Al concentration gradient (50 at% Al at the surface, down to 38 at% Al at the IDZ/bondcoat interface). The  $\beta$ -NiAl coating was about 26µm thick.

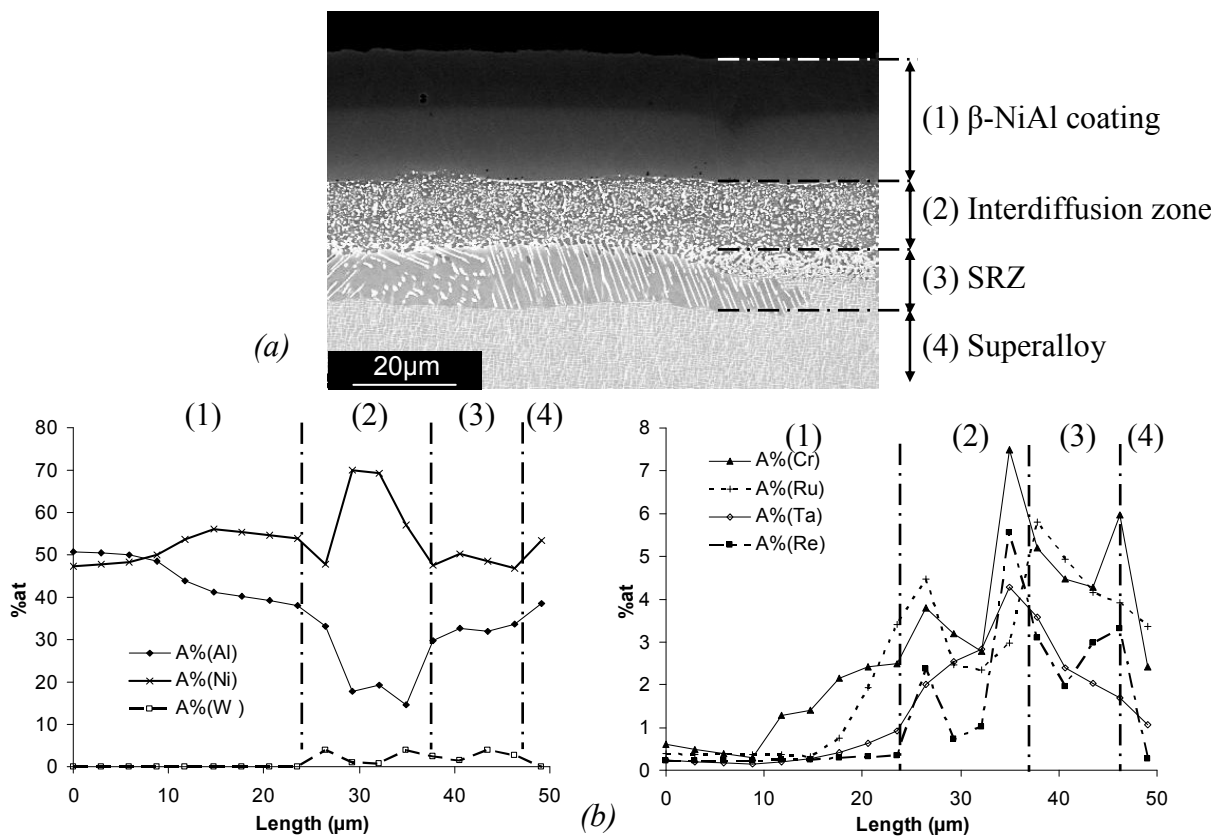


Fig. 2. Cross sections of an aluminised MCNG (a) and associated concentration profiles (b)

**With diffusion barrier.** The DB zone consisted of two different parts as seen in Fig. 4. The first part near the superalloy was 5  $\mu\text{m}$  thick and was composed of refractory element (W, Ta, Re) precipitates in a  $\beta$ -NiAl matrix. The outer part of the DB was only composed of W precipitates in  $\beta$ -NiAl matrix. This zone was 10  $\mu\text{m}$  thick. According to the NiAlW ternary phase diagram [8], W is not very soluble in the  $\beta$ -NiAl. The  $\beta$ -NiAl protective coating had also an Al concentration gradient and had a thickness (27  $\mu\text{m}$ ) close to the thickness of the sample without DB. The presence of a DB had no influence on the quantity of Al added during the aluminisation step.

The main differences between the two samples after aluminisation are the alloying-element concentrations in the  $\beta$ -NiAl and the development of SRZ. Concentration profiles in Fig. 3 and 4 show that alloying-element concentrations are lower in the bondcoating of the sample with DB than in the one of the sample without DB. Moreover, the sample with DB did not develop any SRZ during aluminisation.

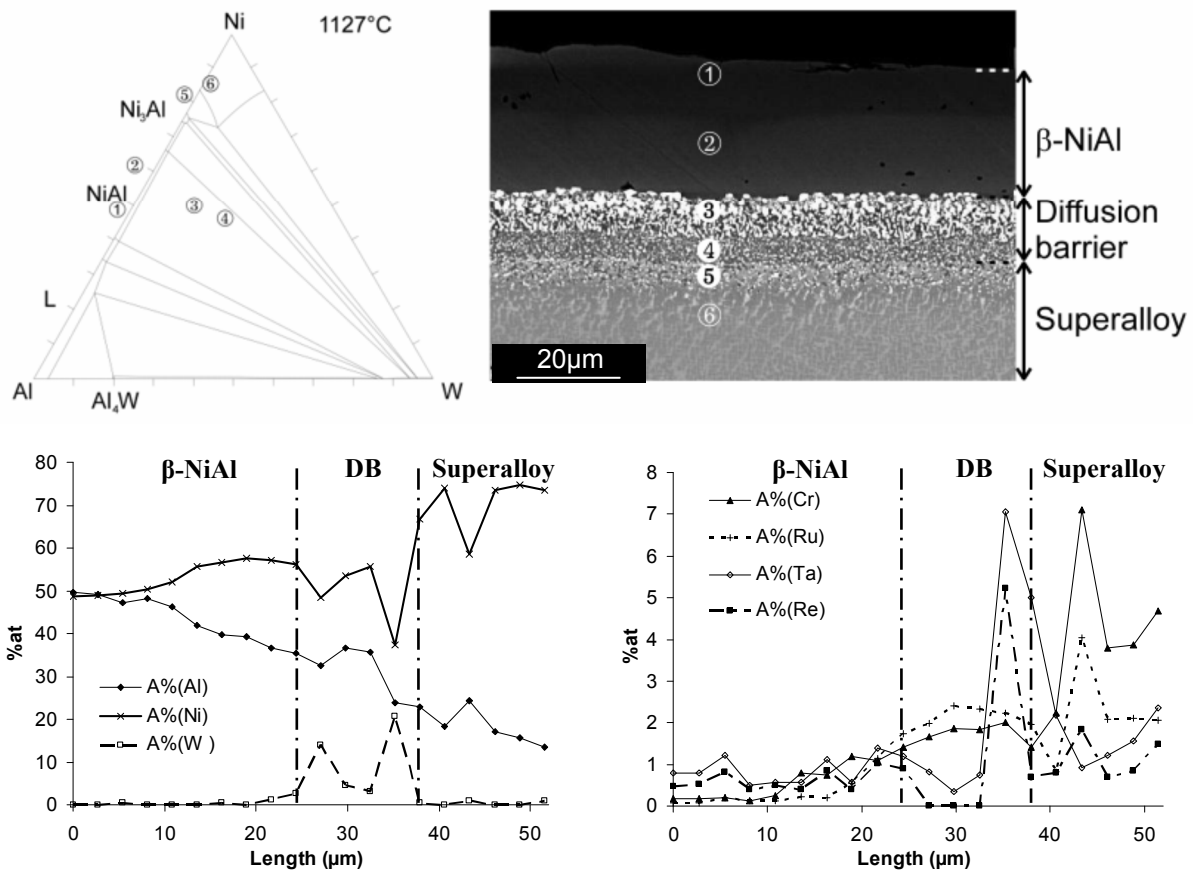


Fig. 3. NiAlW ternary phase diagram [8], cross section and concentration profiles of the aluminised MCNG with diffusion barrier

These results suggest that the establishment of the DB occurred during aluminisation. Ni from the NiW coating avoided using only Ni from the superalloy to form the  $\beta$ -NiAl bondcoating. In parallel, Al diffusion from the coating to the superalloy was slowed, as suggested by the absence of SRZ. The diffusions of Ru and Cr from the superalloy to the bondcoating were modified; however, the DB was not totally continuous after aluminisation.

### Isothermal Oxidation

**Oxidation kinetics** Isothermal oxidation tests were performed during 50 h at 1100°C on the samples without and with DB. The parabolic rate constants ( $k_p$ ) were determined [7] and are reported on the Arrhenius diagram (Fig. 5). This diagram shows the range of  $\text{Cr}_2\text{O}_3$  scaling kinetics obtained by Hindam & Whittle [10] and the  $\theta$ - $\gamma$  and  $\alpha$ - $\text{Al}_2\text{O}_3$  scaling kinetics obtained by Brumm & Grabke on single crystal  $\beta$ -NiAl [11]. Isothermal oxidation tests performed on the present NiAl coatings present two regimes: a transient one followed by a permanent one. The  $k_p$  calculated in the transient regime of the two samples, with and without DB, are in good agreement with the  $k_p$  values of  $\theta$ - $\text{Al}_2\text{O}_3$ . However the  $k_p$  calculated in the permanent regime are lower than the  $k_p$  known for the formation of  $\alpha$ - $\text{Al}_2\text{O}_3$  on NiAl. The  $k_p$  calculated for the permanent regime of these two samples, with and without DB, are very close to each other. But  $k_p$  calculated for the transient regime present a large difference. Specifically, the transient regime  $k_p$  calculated for the sample without DB is two times larger than with a DB.

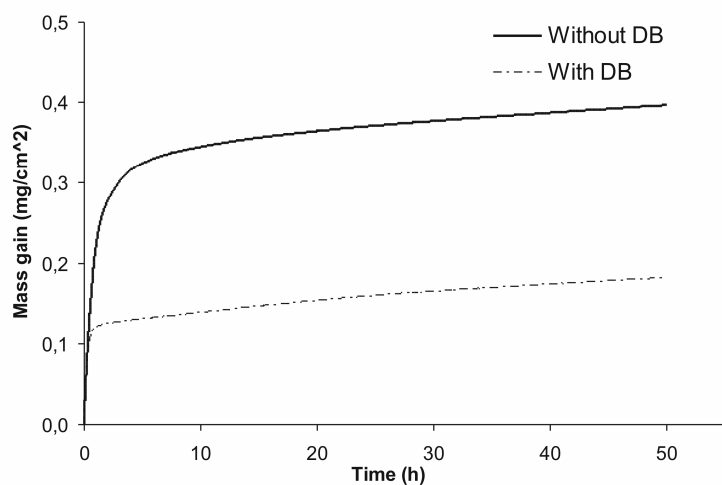


Fig. 4. Mass gain evolution during 50h isothermal tests at 1100°C

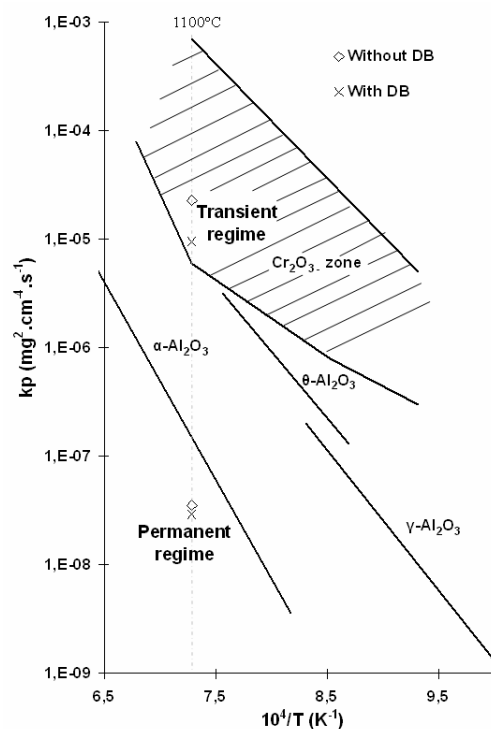


Fig. 5. Oxidation rate constants at 1100°C reported on an Arrhenius diagram

The other main difference between the samples with and without a DB is the transient regime duration. This regime was about 7h long without a DB and 2h long with a NiW DB. The transformation of  $\gamma$  or  $\theta$ -Al<sub>2</sub>O<sub>3</sub> to  $\alpha$ -Al<sub>2</sub>O<sub>3</sub> seemed to happen earlier in systems with a DB. These two differences have a consequence on the oxide-scale thickness. The calculated oxide scale thickness obtained from the mass gain after 50h at 1100°C was 1.95 $\mu$ m for the sample without a DB (1.62 $\mu$ m for the transient regime) and 0.90 $\mu$ m for the sample with a DB (0.60 $\mu$ m for the transient regime).

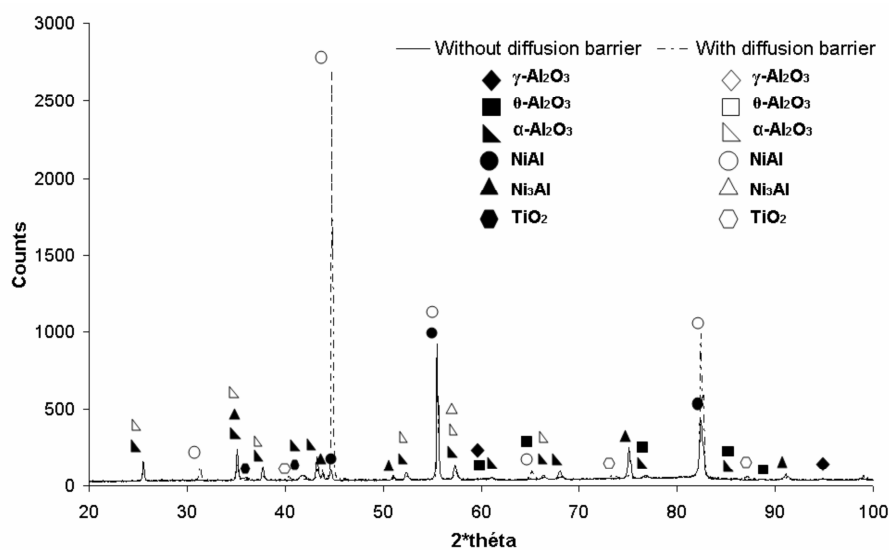


Fig. 6. XRD analyses of "superalloy + NiAl Bondcoat" system with and without NiW diffusion barrier, oxidized 50h at 1100°C



**XRD analysis.** The XRD analysis of the sample without a DB showed weak peaks of transient alumina while analysis of the sample with a DB did not show these peaks. These analyses suggest also that the transition  $\gamma\text{-}\theta\text{-Al}_2\text{O}_3 \rightarrow \alpha\text{-Al}_2\text{O}_3$  occurred faster in the presence of a DB. We can also observe that  $\beta\text{-NiAl}$  peaks are more intense (and  $\gamma'\text{-Ni}_3\text{Al}$  peaks less intense) for the sample with a DB. This can be related to the lower oxidation kinetics observed with a DB during the transient stage.

**Surface observations.** Observation of sample surfaces after oxidation showed a significant difference in oxide-spallation behaviour according the presence or not of a DB (Fig. 7 – (a) (c)). Moreover the oxide surface morphology for the sample without a DB was closer of transient alumina, suggesting that the  $\gamma\text{-}\theta\text{-Al}_2\text{O}_3 \rightarrow \alpha\text{-Al}_2\text{O}_3$  transition occurred later in this case (Fig. 7 – (b) (d)). Fig. 7 – (e) shows an oxide-scale zone of the sample without a DB. This zone spalled at high temperature as indicated by "re-oxidation" that occurred on this zone. Fig. 7 – (f) presents a spalled oxide zone which was not reoxidised. This zone consists of equiaxed  $\alpha\text{-Al}_2\text{O}_3$  grains imprints. Fig. 7 – (g) and (h) present oxide-scale zones of the sample with DB. These zones represent a large proportion of the oxidised sample surface. Cavities can be observed on these zones.

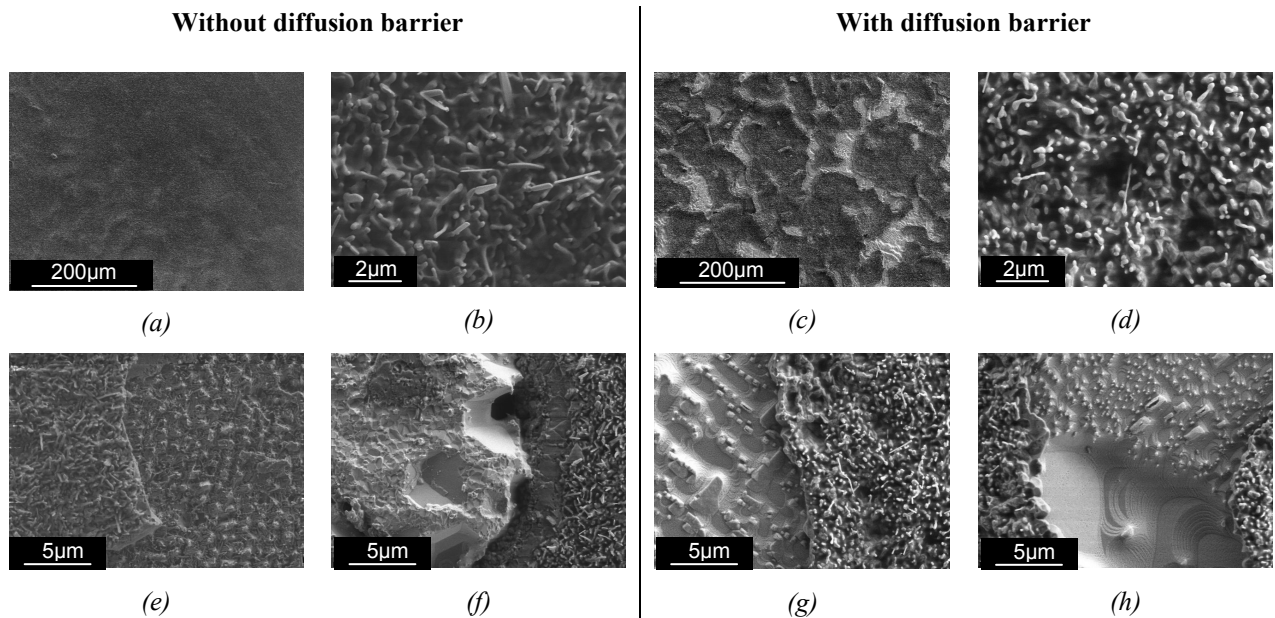


Fig. 7. SEM observations of the oxide surface morphologies after 50h at 1100°C

During isothermal oxidation, the sample with a DB had a shorter transient regime and slightly lower oxidation rate in the permanent regime than the sample without a DB. In a 50h test at 1100°C, the diffusion barrier had a more important influence during the first hours of oxidation than for the following ones. The  $\gamma\text{-}\theta\text{-Al}_2\text{O}_3 \rightarrow \alpha\text{-Al}_2\text{O}_3$  transition occurred earlier with a DB as seen with the kinetics, XRD and oxide morphology. A larger oxide-spalled surface is also observed for the sample with DB. This is in agreement with Cadoret *et al.* [12] and Vialas *et al.* [13] who suggested that a delayed  $\theta\text{-Al}_2\text{O}_3 \rightarrow \alpha\text{-Al}_2\text{O}_3$  transition reduces the level of compressive stress in the alumina scale during a longer period.

**Cross section observations.** Fig. 8 – (a) shows three different zones above the aluminised superalloy without a DB after 50h of oxidation at 1100°C. First, the SRZ developed in about 80% of the superalloy periphery and was approximately 20µm deep. Also, the phases present in the IDZ did not change during isothermal oxidation but their thicknesses increased. Finally, the bondcoating was still 25µm thick but now composed of  $\gamma'\text{-Ni}_3\text{Al}$  in a  $\beta\text{-NiAl}$  matrix. Fig. 8 – (b) also shows three different zones above the aluminised superalloy coated with a DB. First the IDZ was

approximately 20 $\mu\text{m}$  thick. Then, there is the DB zone which can be divided in two parts. The inner part is composed of W precipitates associated with refractory elements (Re, Cr, Ta) and  $\gamma'$ -Ni<sub>3</sub>Al in a  $\beta$ -NiAl matrix. This part was about 5 $\mu\text{m}$  thick. The outer part was composed of the same phases as the inner one but the precipitates were denser and its thickness was 10 $\mu\text{m}$ . The thicknesses of these two parts did not change during the oxidation test. Moreover it can be noticed that the bondcoating presents a very small amount of  $\gamma'$ -Ni<sub>3</sub>Al in its  $\beta$ -NiAl matrix compared to the sample without a DB. Finally the sample with a DB did not form any SRZ before and after the 50h isothermal oxidation test at 1100°C.

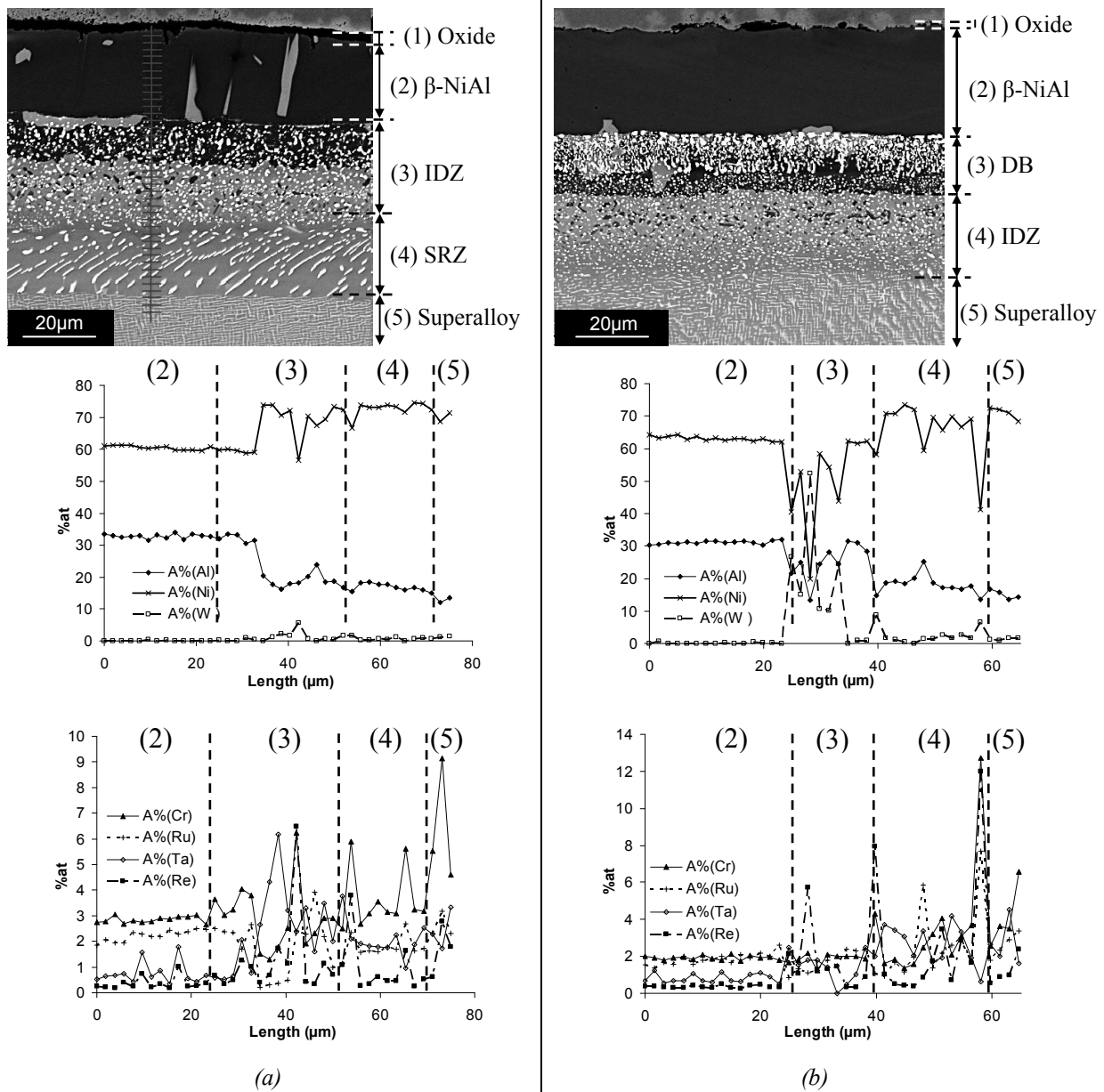


Fig. 8. BSE cross section observations and EDS concentration profiles after 50h at 1100°C of samples without DB (a) and with DB (b)

After oxidation the bondcoating without a DB exhibits a larger part of Ni<sub>3</sub>Al than the bondcoating with a DB. A first rough estimation gives 8 vol% of  $\gamma'$  in the bondcoating without a DB and 2 vol% in the bondcoating with a DB. This observation is in good agreement with the XRD analysis. In the oxidised samples, the composition of  $\beta$ -NiAl is approximately constant (30-32%at Al). Then, the total quantity of Al present in the bondcoating is directly related to the Ni<sub>3</sub>Al phase proportion. The more important proportion of Ni<sub>3</sub>Al in the bondcoating without a DB suggests that a larger quantity

of Al has been used by oxidation and interdiffusion. In addition the fact that no SRZ developed in the sample with DB suggests also that less Al diffused from the bondcoating to the superalloy than in the sample without a DB.

### Conclusions

The efficiency of a Ni<sub>75</sub>W<sub>25</sub> electrolytic coating annealed 16h at 1100°C acting as a DB between a MCNG superalloy and a β-NiAl bondcoating has been studied. After isothermal oxidation testing for 50h at 1100°C, the behaviours of the as-aluminised specimens with and without a DB were compared. The microstructure and the oxide scale formed after oxidation were also compared. The results may be summarized as follows:

1. After aluminisation step of the NiW electrolytic coating annealed 16h at 1100°C, a W-precipitates-rich layer between the superalloy and the bondcoating was created. In accordance with NiAlW ternary phase diagram, these precipitates are insoluble in their β-NiAl matrix. The DB avoids the development of SRZ without modifying the thickness and the composition of the bondcoating.
2. The transient oxidation stage was longer for the specimen without a DB, resulting in a doubled mass gain in comparison with the coating with a DB, i.e. a higher Al consumption. After the transient stage, the oxidation rate constants were very similar for the two samples.
3. The sample without a DB formed SRZ after aluminisation (about 50% of the superalloy periphery) that increased during isothermal oxidation (to about 80%).
4. The sample with a DB did not present any SRZ before and after the 50h isothermal oxidation test at 1100°C.
5. Lower transient stage oxidation and lower interdiffusion with the DB led to less β-NiAl → γ'-Ni<sub>3</sub>Al transformation.
6. The DB limits some alloying elements diffusion from the substrate to the surface, especially Cr and Ru.
7. After 50h isothermal exposure at 1100°C, the system with a DB showed increased alumina scale spallation. Nevertheless, long-term oxidation and thermal cycling are necessary to evaluate the long-term effect of the DB on the durability of the systems. Indeed, 50h at 1100°C is not sufficient to reduce the Al level under a critical concentration in the bondcoating, and cyclic oxidation is necessary to evaluate the effect of delayed β-γ' transformation. Alloying of the coating with Pt and/or reactive elements may also hide the negative effect of DB on spalling.

### References

- [1] P. Caron, T. Khan, *Aerospace Science and Technology*. Vol. 3 (1999), p. 513-523
- [2] T. Narita, K.Z. Thosin, L. Fengqun, S. Hayashi, H. Murakami, B. Gleeson, D. Young, *Materials and Corrosion*. Vol. 56 (2005), p. 923-929
- [3] J.A. Haynes, Y. Zhang, K.M. Cooley, L. Walker, K.S. Reeves, B.A. Pint, *Surface & Coatings Technology*, Vol. 188-189 (2004), p. 153-157
- [4] M.P. Bacos, P. Josso, FR Patent 2881439. (2006)
- [5] S. Walston, A. Cetel, R. MacKay, K. O'Hara, D. Duhl, R. Dreshfield, *Superalloys* (2004), p. 15-24
- [6] O. Lavigne, J. Benoist, P. Caron, C. Ramusat, *Turbine Forum* (2006)
- [7] D. Monceau, B. Pieraggi, *Oxidation of Metals*. Vol. 50 (1998), p. 5-6
- [8] L. Kaufman, H. Nesor, *Canadian Metallurgical Quarterly*, Vol. 14 (1975), p. 221-232
- [9] M. Reid, M.J. Pomeroy, J.S. Robinson, *Journal of Materials Processing Technology*. Vol. 153-154 (2004), p. 660-665
- [10] H. Hindam, D.P. Whittle, *Oxidation of Metals*, Vol. 18 (1982), p. 245
- [11] M.W. Brumm, H.J. Grabke, *Corrosion Science*, Vol. 33 (1992), p. 1677
- [12] Y. Cadoret, D. Monceau, M.-P. Bacos, P. Josso, V. Maurice, P. Marcus, *Oxidation of Metals*, Vol. 64 (2005), p. 185-205
- [13] N. Vialas, D. Monceau, *Oxidation of Metals*, Vol. 66 (2006), p. 30